NeuroImage: Clinical 47 (2025) 103825

Contents lists available at ScienceDirect

NeuroImage: Clinical

journal homepage: www.elsevier.com/locate/ynicl

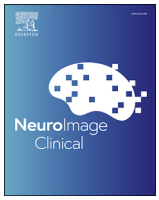

The role of contralesional regions for post-stroke movements revealed by dynamic connectivity and TMS interference

Lukas Hensel [a], Anna K. Bonkhoff [b], Theresa Paul [a], Caroline Tscherpel [c], Fabian Lange [a], Shivakumar Viswanathan [d], Lukas J. Volz [a], Simon B. Eickhoff [e,f], Gereon R. Fink [a,d], Christian Grefkes [c,d,*]

[a] Faculty of Medicine and University Hospital Cologne, Department of Neurology, University of Cologne, Cologne, Germany
[b] J. Philip Kistler Stroke Research Center, Massachusetts General Hospital, Harvard Medical School, Boston, MA, USA
[c] Goethe University Frankfurt, Frankfurt University Hospital, Department of Neurology, Frankfurt am Main, Germany
[d] Cognitive Neuroscience, Institute of Neuroscience and Medicine (INM-3), Research Centre Jülich, Jülich, Germany
[e] Institute of Systems Neuroscience, Medical Faculty, Heinrich Heine University Düsseldorf, Düsseldorf, Germany
[f] Institute of Neuroscience and Medicine, Brain & Behaviour (INM-7), Research Centre Jülich, Jülich, Germany

ARTICLE INFO

Keywords:
Stroke
Motor performance
Dynamic functional connectivity
Network segregation
rTMS

ABSTRACT

Connectivity changes after brain lesions due to stroke are tightly linked to functional outcome. Recent analyses of fMRI time series indicate that dynamic functional network connectivity (dFNC), reflecting transient states of connectivity may capture network-level disruptions distant to the lesion site. Yet, the relevance of such dynamic connectivity patterns for motor recovery remains unclear. We, therefore, combined the analysis of static and dFNC and a repetitive transcranial magnetic stimulation (rTMS) lesion approach, to test whether dFNC provides region-specific insight into motor system reorganization after stroke. We focused on the contralesional primary motor cortex (M1) and anterior intraparietal sulcus (aIPS), two regions previously shown to modulate motor performance post-stroke in a time dependent manner. In 18 individuals in the chronic phase after stroke (with either persistent or recovered deficits) and 18 healthy participants, we analyzed static and dynamic resting-state connectivity. We then applied online rTMS intereference over contralesional aIPS and M1 during hand movement tasks to assess region-specific contributions to motor behavior. Consistent with previous studies, dFNC states were associated with persisting motor deficits, whereas static connectivity was not associated with motor outcome. dFNC but not static connectivity was associated with residual motor deficits and explained TMS-induced behavioral changes, when applying rTMS over contralesional M1. For contralesional aIPS, both static and dynamic connectivity were linked to TMS effects.

This indicates that dFNC – more than static connectivity – contains information on the functional relevance of brain regions for motor outcome, specifically contralesional M1. Our results highlight the added value of temporal network analysis in understanding mechanisms of stroke recovery mechanisms.

1. Introduction

Motor deficits following ischemic stroke are a major cause for acquired long-term disability (Kessner et al., 2019), raising the interest in personalized treatment strategies based on individual assessments of the motor system (Bonkhoff and Grefkes, 2022; Grefkes and Fink, 2016; Koch and Hummel, 2017; Morishita and Hummel, 2017). Recovery of motor function is not only driven by local changes near the lesion but also by change of interactions between distant brain areas (Baldassarre et al., 2016; Carter et al., 2010; Finger et al., 2004; Golestani et al., 2013;

Abbreviations: ANOVA, Analysis of Variance; aIPS, Anterior Intraparietal Sulcus; ARAT, Action Arm Research Test; BIC, Bayesian Information Criterion; BOLD, Blood Oxygenation Level Dependent; dFNC, Dynamic Functional Network Connectivity; FDR, False Discovery Rate; FWHM, Full Width at Half Maximum; IQR, Interquartile Range; M1, Primary Motor Cortex; MNI, Montreal Neurological Institute; fMRI, Functional Magnetic Resonance Imaging; ICA, Independent Component Analysis; NIHSS, National Institutes of Health Stroke Scale; PCA, Principal Component Analyses; ROI, Region of Interest; rTMS, Repetitive Transcranial Magnetic Stimulation; SMA, Supplementary motor area; SPM, Statistical Parametric Mapping; TMS, Transcranial Magnetic Stimulation.

* Corresponding author at: Department of Neurology, University Hospital Frankfurt, Goethe University, Frankfurt am Main, Germany.
E-mail address: Grefkes-Hermann@em.uni-frankfurt.de (C. Grefkes).

https://doi.org/10.1016/j.nicl.2025.103825
Received 4 February 2025; Received in revised form 31 May 2025; Accepted 9 June 2025
Available online 11 June 2025

Grefkes and Fink, 2014; Monakow, 1914; Wang et al., 2010). In particular, interhemispheric connections between the contralesional primary motor cortex (M1) and anterior intraparietal sulcus (aIPS) have been demonstrated to play key roles in post-stroke motor adaptation. M1 governs direct motor output, aIPS supports higher-order visuomotor integration essential for complex motor tasks such as grasping (Binkofski et al., 1999; Grefkes and Fink, 2005). Both regions show decreased interhemispheric connectivity in the acute phase after stroke, which re-emerges in the following weeks along motor recovery (Meer et al., 2010; Park et al., 2011; Volz et al., 2016). Interfering with contralesional M1 and aIPS using rTMS after stroke has demonstrated that these regions are involved in movements of the stroke-affected hand (Lotze et al., 2006; Tscherpel et al., 2020b; Werhahn et al., 2003), suggesting that interhemispheric connectivity between M1 and aIPS is relevant for residual motor capacity. Yet previous fMRI analyses have typically focused on average connectivity estimates measured over several minutes (static connectivity).

Importantly, motor adaptation after stroke likely depends on the brain's flexibility to reconfigure its networks (Bonkhoff et al., 2020a), switching between integrated states for coordinated output and segregated states for specialized processing (Shine et al., 2016; Wu et al., 2024). Such time-sensitive network dynamics are captured by the 'dynamic' functional connectivity (dFNC) approach (Allen et al., 2014; Chang and Glover, 2010; Damaraju et al., 2014), which uses a sliding window techniques to reveal transitions between connectivity states. Assessing dFNC in patients with acute stroke has revealed that temporally distinct connectivity states are associated with different levels of acute motor impairment (Bonkhoff et al., 2020a) and recovery (Bonkhoff et al., 2021a). Patients with more severe symptoms spent more time in highly segregated network states, where functionally related sensorimotor regions—including M1 and premotor areas—were strongly interconnected, but showed only weak or negative connectivity with other networks such as frontoparietal, subcortical, or cerebellar regions (Bonkhoff et al., 2020a, 2021b). However, it remains open whether these transient connectivity states during rest reflect neural processes involved in maintaining motor performance in the stroke-damaged brain. To causally test the roles of single regions within the reorganized motor system after stroke, repetitive TMS has often been applied over motor-related regions during the execution of motor tasks (online-rTMS interference) (Hensel et al., 2021; Lotze et al., 2006; Tscherpel et al., 2020b; Volz et al., 2017). For example, M1 and aIPS negatively influence hand movements in the first two weeks after stroke, which for contralesional aIPS may persist several months later (Tscherpel et al., 2020b; Volz et al., 2017).

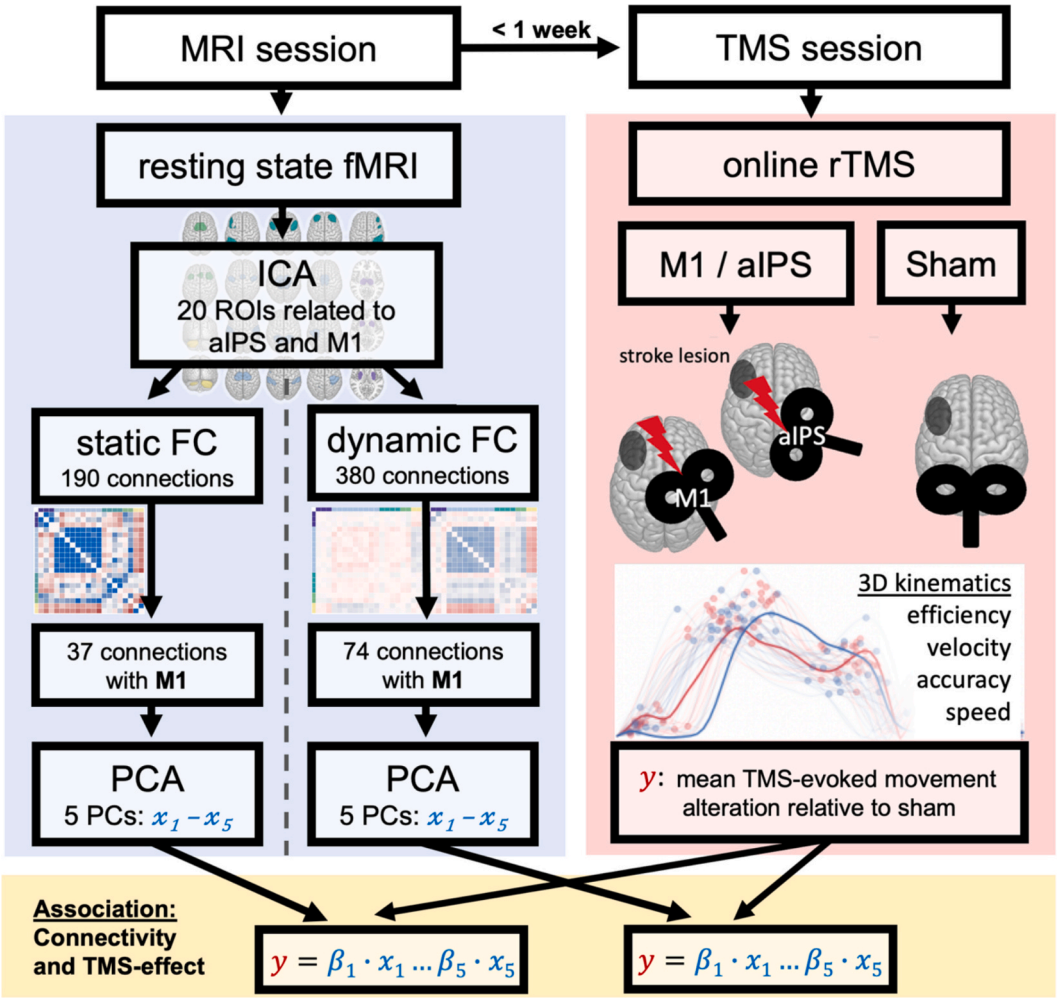

Fig. 1. Relating static and dynamic connectivity to the role of a region of interest (e.g. M1). Left (blue): dimension reduction of resting state fMRI data. Motor-related connections, which are connected to the investigated region of interest (M1 or aIPS) are transformed into an equal number of principal components for static and dynamic functional connectivity. Right (red): Effects on poststroke movements by interfering with the region of interest (M1 or aIPS) using online-rTMS. Bottom (yellow): Regression analyses test for a relationship of dynamic and static functional connectivity with the causal motor contributions of contralesional M1 and aIPS, respectively. ICA = independent component analysis, ROIs = regions of interest. FC = functional connectivity, M1 = primary motor cortex, PCA = principal component analysis. (For interpretation of the references to color in this figure legend, the reader is referred to the web version of this article.)

Taken together, accumulating evidence indicates that dFNC holds information about stroke outcome, (Bonkhoff et al., 2020a, 2021a, 2021b), and online-rTMS can probe how these dynamic patterns relate to the functional contributions of contralesional M1 and aIPS. Here, we aimed to (1) replicate prior findings that dFNC distinguishes patients with lower versus higher motor outcome, and (2) determine whether dFNC within contralesional M1 and aIPS better explains their roles in hand motor performance than static connectivity. To test this, we re-analyzed data from a prior study where 18 individuals with recovered or persistent motor deficits in the chronic phase after stroke and 18 healthy participants underwent online-rTMS after an fMRI session (Fig. 1) (Hensel et al., 2023). From this data, contributions of contralesional (i.e. ipsilateral to the moving hand) M1 and aIPS for hand movements upon brief rTMS pulse trains were available for all participants as well as resting fMRI for the estimation of dFNC.

Both contralesional M1 and contralesional IPS are assumed to contribute to motor function through connections with the ipsilesional hemisphere, especially in patients with lower motor outcome (Grefkes et al., 2010; Hensel et al., 2023; Turton et al., 1996; Werhahn et al., 2003). We hypothesized that the dFNC of these areas within their respective networks is linked to the differing effects of M1 and aIPS on motor behaviour under rTMS interference. To test this hypothesis, we first sought to replicate the dFNC-related findings from prior studies (Bonkhoff et al., 2020a, 2021a, 2021b) by comparing dFNC between patients with lower and higher outcome, assuming that stroke-related abnormalities of connectivity are more sensitively detected using dFNC, compared to static connectivity. Then, we tested whether dFNC contains information about the differing roles of contralesional M1 and aIPS on recovered hand motor function after ischemic stroke (Fig. 1). If transient connectivity states are relevant to post-stroke motor outcomes, then models based on dFNC were expected to explain the contributions of contralesional M1 and aIPS better than equivalent models based on static connectivity.

2. Materials and methods

2.1. Participants

Data were extracted from a previous study (Hensel et al., 2023) including 18 individuals in the chronic phase after first-ever ischemic stroke (> six months after onset) with unilateral hand motor deficit and 18 healthy controls tested at the Department of Neurology, University Hospital Cologne. The original study was designed to probe the causal contributions of contralesional M1 and aIPS to hand motor performance using time-locked online-rTMS during three kinematic tasks (finger-tapping, reach-to-grasp, reach-to-point). However, in the previous study, we did not consider any relationship of TMS effects with dynamic connectivity, which were exclusively computed for the present study. Inclusion criteria were an age between 40–90 years, no contraindications to TMS or MRI, absence of cerebral hemorrhage, no bihemispheric infarcts and the absence of severe aphasia, apraxia, or neglect. Demographic and clinical details of the cohort are provided in Table 1.

Following the original study for the current data (Hensel et al., 2023), the patients were divided into two sub-groups based on their movement kinematics in the three tested tasks, namely, finger-tapping, reach-to-grasp and reach-to-point (see Supplementary methods for a summary of the grouping rationale). The two subgroups are referred to here as the *lower motor outcome* (LMO) (n = 9) and the *higher motor outcome* (HMO) (n = 9) groups respectively. The kinematic assessment of individual-specific movements (patients and healthy controls) yielded a Motor Performance Score that served as a data-driven and clinically correlated measure of general motor performance of the upper limb for each individual. (Hensel et al., 2023). Motor performance of healthy participants (1.05 ± 0.67) and patients with high outcome (0.28 ± 0.70) was significantly higher compared to patients with low outcome (–2.39 ± 1.12), as indicated by independent t-tests (HC and HMO: t(11.0) = 8.50, P < 0.001; HMO and LMO: t(13.4) = 6.08, P < 0.001). Although performance in the higher outcome group was close to the healthy controls, significant differences in hand kinematics were still detectable (HC and HMO: t(15.6) = 2.76, P = 0.014). Notably, a group-level analysis of TMS effects in these cohorts was already reported in Hensel et al. (2023). The present study focuses instead on explaining individual differences in TMS effects using dynamic and static functional connectivity.

Table 1
Sample characteristics.

	Stroke Patients	Healthy Controls	P
Age [y]	66.2 ± 13.0	66.5 ± 7.2	*0.937*[1]
Gender [m/f]	(13/5)	(12/6)	*0.717*[2]
Lesion side [l/r]	(8/10)		
EHI	0.89 ± 0.15	0.78 ± 0.24	*0.119*[1]
Months post-stroke	30.4 ± 20.7		
ARAT affected Hand*	55.5 (45.3–57.0)	57.0 (57.0–57.0)	***0.007***[3]
NIHSS*	1.5 (1.0–2.8)	0.0 (0.0—0.0)	***<0.001***[3]
NIHSS (acute phase)*	7.0 (6.0–9.8)		
NIHSS upper limb score*	1.0 (0.0–1.0)	0.0 (0.0—0.0)	***<0.001***[3]
NIHSS upper limb score (acute phase)*	2.5 (2.0–3.0)		

EHI: Edinburgh Handedness Inventory, NIHSS: National Institutes of Health Stroke Scale, ARAT: Action Research Arm Test.
* nonparametric data is described by medians and interquartile range; n.a. = not applicable (due to identical values across all subjects and groups)
[1]t-test, [2]Chi-squared-test, [3]U-test

All participants provided written informed consent before inclusion. The study was approved by the local ethics committee at the University of Cologne (file no: 17–244) and was performed in compliance with the Declaration of Helsinki (1969, last revision 2013).

2.2. Experiment

2.2.1. fMRI acquisition and preprocessing

In the first experiment session, structural and functional MRI (task and rest) was recorded (Fig. 1). The task-fMRI was used to localize peak BOLD activations as stimulation targets in the second session. Resting- and task-fMRI data were preprocessed using Statistical Parametric Mapping (SPM12; The Wellcome Centre for Human Neuroimaging, London, UK, https://www.fil.ion.ucl.ac.uk) implemented in Matlab version 2016b (The Mathworks Inc.; MA, USA). Details on data acquisition are reported in the supplementary material. From a total of 450 EPI volumes per participant, the first 10 EPI scans were excluded avoiding noise from magnetic field saturation. To arrange the lesions uniformly in the left hemisphere, scans from individuals with right-hemispheric lesions (n = 10) and matched healthy controls (n = 9) were flipped along the midsagittal plane (Schulz et al., 2016; Steiner et al., 2021). Lesion masks were drawn based on T2 images using MRIcron (https://www.sph.sc.edu/comd/rorden/Mricron).

The task-data were preprocessed at the single subject level to localize rTMS targets, while resting-state fMRI data were prepared for the second-level analysis of functional connectivity (Hensel et al., 2021). Specifically, both task- and resting-fMRI images were first corrected for head movement by spatial realignment to the mean image. However, only resting-state fMRI images were spatially normalized into standardized MNI-space using the 'unified segmentation' procedure (Ashburner and Friston, 2005) after masking lesioned tissue. Consistent with previous work, the normalized resting-state images were smoothed using a Gaussian kernel with FWHM of 8 mm (Bonkhoff et al., 2020a; Hensel et al., 2021).

2.2.2. Online-rTMS

In a second session within one week after the fMRI, the identified targets (contralesional M1, contralesional aIPS, and ipsilesional aIPS)

were tested by online-rTMS interference during three movement tasks of differing complexity (tapping, pointing, grasping) (Hensel et al., 2023). Note that only performance related to M1 and aIPS in the contralesional hemisphere was evaluated in the current study since the study aimed to investigate contributions of motor regions distant to the stroke lesion. Hand movements were tested during online-rTMS over these contralesional regions (M1, aIPS), i.e. ipsilateral to the moving hand. Moreover, a sham (control) stimulation was applied tilting the coil over the parieto-occipital vertex, so that the TMS focus was located outside neural tissue. TMS was applied using a Magstim Super Rapid2 system (The Magstim Co. Ltd, Whitland, UK) equipped with a Magstim 70 mm Double Air Film Coil. The exact location of contralesional aIPS was defined by the local peak of fMRI activation during the finger tapping localizer task, the contralateral M1 activation was defined by the electrophysiological hotspot determined by motor evoked potentials in the first interosseous (FDI) muscle (Hensel et al., 2023).

Consistent with previous studies (Hensel et al., 2021; Lotze et al., 2006; Tscherpel et al., 2020b; Volz et al., 2017), 10 Hz rTMS was applied at 90 % of the resting motor threshold to transiently perturb neural processing in each region of interest, time-locked to behavioral recordings of hand movements. These comprised (i) finger-tapping, (ii) rapid pointing between to targets, and (iii) a reach-grasp-lift task. Using the software Presentation® (Version 9.9, Neurobehavioral Systems, USA, https://www.neurobs.com), trains of 16 TMS pulses were triggered starting at the beginning of each motor task, cued by an auditory and visual signal. Execution of one task lasted 1.6 s for finger-tapping, and 2.0 s for pointing and reach-grasp-lift, with breaks of 5.5 s. The TMS coil position changed every seven trials in a pseudo-randomized order so that each of the conditions was assessed for an equal number of trials during each quarter of the experiment.

All participants repeated each of these tasks 28 times per rTMS condition. The online-rTMS effect on one region (M1 or aIPS) was computed by comparing hand movements during each real rTMS with the performance during sham rTMS (Hensel et al., 2023), referred to as "Mean Movement Alteration" induced by online-rTMS.

2.3. Connectivity between motor regions

2.3.1. Component (region of interest) selection

As shown in Fig. 1 (left panel), preprocessed resting-state fMRI data were first entered into a constrained high-dimensional independent component analysis (ICA) to extract intrinsic components as regions of interest (ROIs) for the functional connectivity analysis (Du and Fan, 2013; Lin et al., 2010). The ICA was constrained by a total of 100 components estimated from resting state functional MRI data of 405 healthy controls (Allen et al., 2014; Calhoun et al., 2001), avoiding spatial bias from stroke lesions while gaining robustness to noise by accounting for each participant's functional properties (Du et al., 2016; Salman et al., 2019). Hence, spatial maps and time courses were obtained for each participant using the back-reconstruction approach (GICA) (Calhoun et al., 2001). We excluded components not situated mainly in gray matter and showing low ratios of low- to high-frequency spectra, indicating noise rather than neural signal. To further remove potential artifacts not captured by the ICA, components' time courses were detrended, despiked using 3Ddespike (Cox, 1996), filtered by a fifth-order Butterworth low-pass filter with a high-frequency cut-off of

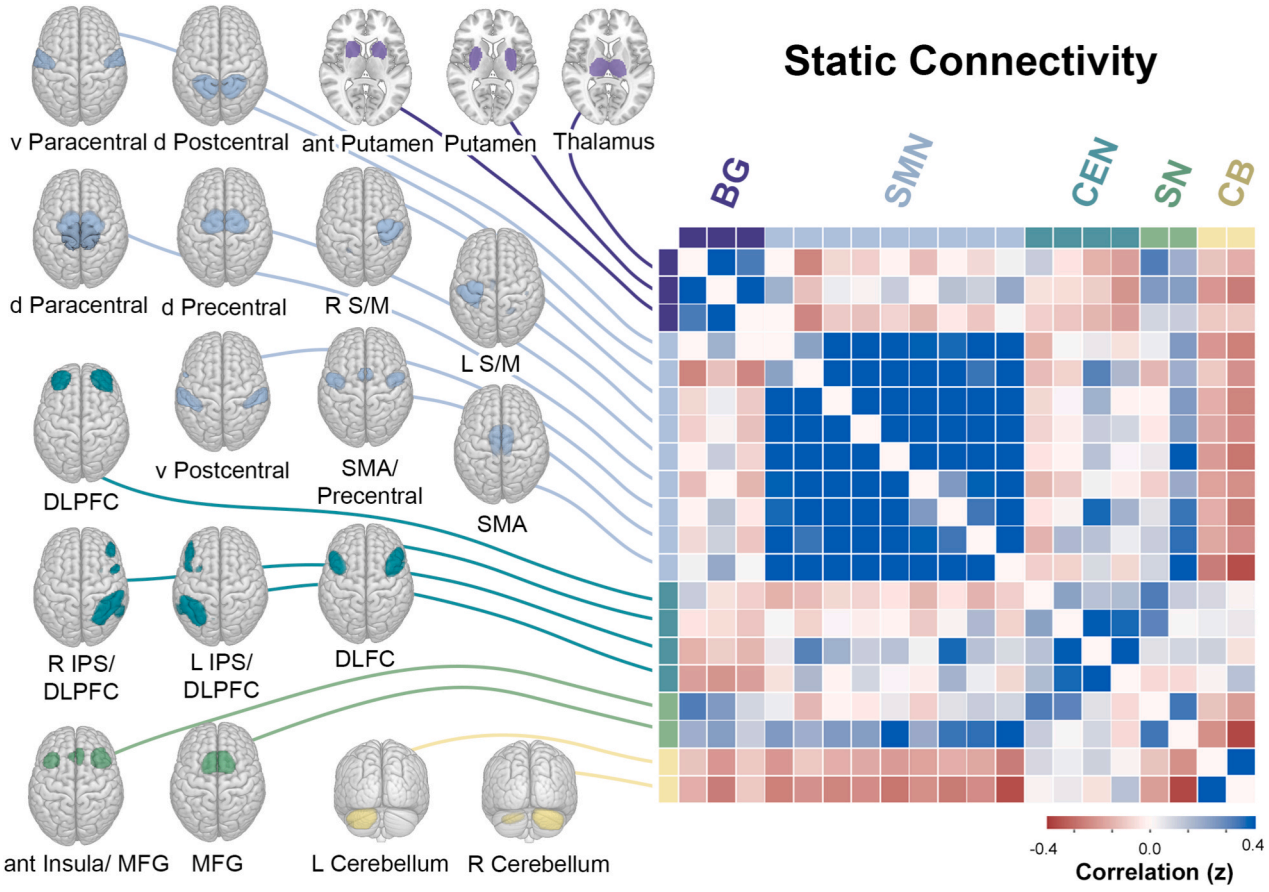

Fig. 2. Motor-related network. Left: Spatial maps of 20 ICA components reflecting intrinsic connectivity networks across patients and healthy participants, color coded by affiliation to larger-scale networks. BG (dark purple) = basal ganglia network, SMN (light blue) = sensorimotor network, CEN (dark green) = central executive network, SN (light green) = saliency network, CB (yellow) = cerebellar network. Right: Matrix of static connectivity values between all components of all participants (patients and healthy controls). (For interpretation of the references to color in this figure legend, the reader is referred to the web version of this article.)

0.15 Hz, and normalized for variance (Rachakonda et al., 2007).

We selected components comparable to our previous dFNC studies on the motor system after stroke (Bonkhoff et al., 2020a, 2021a), aiming to investigate the motor network in which M1 and aIPS are integrated to obtain a neurobiologially plausible model of brain regions involved in the generation of hand movements. We then used online-rTMS interference to probe the role of two respective network nodes, i.e. M1 and aIPS, for the control of finger movements and grasping after stroke (Caspers et al., 2012; Culham and Valyear, 2006; Davare et al., 2011; Grefkes and Fink, 2005; Rice et al., 2006) (Fig. 2). In total, 20 components from five motor networks were selected: (i) A basal ganglia network consisted of three components in the anterior Putamen, Putamen, and Thalamus. (ii) A sensorimotor subnetwork consisted of nine components, namely left and right primary sensorimotor cortex, ventral and dorsal paracentral cortex, ventral and dorsal postcentral cortex, dorsal precentral cortex, supplementary motor area (SMA) and a component reflecting both SMA and precentral cortex. (iii) Four components were assigned to the central executive network, associated with higher-level control (Power et al., 2011; Seeley et al., 2007), comprising bilateral frontal poles, dorsolateral frontal cortex, and two components mainly located in the intraparietal sulcus of the right and left hemisphere, respectively. (iv) Moreover, two components in anterior insula and medial frontal gyrus were included as a saliency network (Seeley et al., 2007), mediating motivational processes facilitating motor initiation (Hoffstaedter et al., 2013; Rushworth et al., 2004). (v) Finally, a cerebellar network was defined by a predominantly left- and right-cerebellar component. The identified components served as the common regions of interest to assess (1) static and (2) dynamic function connectivity (left panel, Fig. 2).

2.3.2. Static functional connectivity

Static connectivity was computed using the z-transformed Pearson pairwise correlation of the entire resting-state time-series for every pair of components. This analysis for all of the 20 components yielded 190 connectivity values (20 components * (20 components – 1) / 2 = 190) for each participant. Consistent with previous connectivity studies in stroke (Bonkhoff et al., 2020a, 2021a, 2021b), age, sex, mean framewise translation and rotation were used as independent regressors to correct for physiological variability and within scanner movement.

2.3.3. Dynamic functional connectivity

DFNC between the aforementioned 20 components was analyzed applying a sliding window approach (Allen et al., 2014; Calhoun et al., 2014; Damaraju et al., 2014; Sakoğlu et al., 2010) implemented in the GIFT toolbox (version 4.0, https://trendscenter.org/software/gift/). To reduce spurious fluctuations, average sliding window correlations (ASWC) were computed using a nominal window (40.5 s) and average (50 s) lengths, yielding 328 connectivity matrices (Vergara et al., 2019). Analogous to the static connectivity analysis based on the same 20 components, this resulted in 190 connectivity values for each participant. To correct for effects of no-interest, we included the regressors age, sex, mean framewise translation and rotation. The ensuing dFNC values were Fisher z transformed.

Next, based on all time windows from all subjects, we delineated distinct *connectivity states* using k-means clustering, identifying recurring patterns of functional connectivity across time and subject space (Allen et al., 2014; Calhoun et al., 2014; Lloyd, 1982). As a suitable function for high-dimensional data, the l_1 distance (Manhattan distance) was used to estimate the similarity of each window's connectivity to the cluster centroid. Consistent with previous work (Bonkhoff et al., 2020a; Díez-Cirarda et al., 2018; Fiorenzato et al., 2019), we determined the optimal number of connectivity states using the silhouette measure (Rousseeuw, 1987), the elbow criterion based upon the cluster validity index (Espinoza et al., 2018), and the Gap statistic (Tibshirani et al., 2001), favoring a two-cluster solution (see Supplementary Data). Hence, k-means clustering was re-computed for k = 2, assigning each time window across all participants to one of two clusters, referred to as connectivity states.

2.4. Comparing connectivity between subgroups

2.4.1. Functional connectivity

As described above, static connectivity was depicted in a single state (190 connections) whereas the dynamic connectivity yielded two states (2 x 190 connections). In line with previous dynamic connectivity studies (Bonkhoff et al., 2020a; Fiorenzato et al., 2019), we compared connectivity strengths between groups (healthy, higher outcome, lower outcome) for each of the 190 connections in each connectivity state using one way analyses of variance (ANOVA, $P < 0.05$, FDR-corrected). In case of significant ANOVA results, post hoc t-tests between healthy participants and patient subgroups were performed ($P < 0.05$, FDR-corrected). All FDR-corrections for multiple comparisons were performed using the Benjamini-Hochberg procedure.

2.4.2. Dynamic transition measures

The dynamic transitions between dFNC states were summarized by (1) the *dwell time* (mean time remaining in a given state without transitioning into another), (2) *fraction time* (portion of total time spent in a given state) and (3) *number of transitions* (total number of transitions from any state to another).

Group differences in dwell time were assessed with mixed ANOVAs with the within-subjects factor dFNC STATE (Dynamic connectivity state 1 and 2) and the between-subjects factor GROUP (healthy, higher outcome, lower outcome). Group differences in fraction time and the number of transitions were each conducted by a three-level one way ANOVA with the between-subjects factor GROUP (Bonkhoff et al., 2021b; Rabany et al., 2019; Schwanenflug et al., 2022). One-way ANOVAs were chosen for these measures, since fraction times of two states were precisely symmetrical with fraction times for states one and two always adding up to 1, and the number of transitions only describes one value per participant.

The linear relationship between dFNC and hand motor function across individuals was assessed by computing Pearson correlations between each dynamic connectivity measure (dwell time, fraction time, number of transitions) and the Motor Performance Score, which summarized kinematic measures across all upper limb movements (see Supplementary material, Motor Performance Score).

2.5. Relating connectivity to roles of M1 and aIPS

As illustrated in Fig. 1, associations between static FC and dFNC and the roles of M1 and aIPS for post-stroke movements were separately tested using linear backward regression models with elimination based on the Bayesian information criterion (BIC, k = log(n) with n = 18). Specifically, in each model, the connectivity measures (either static or dynamic) served as input variables whereas outcome variables reflected a regions' contribution to hand movements (either M1 or aIPS). In total, four linear models were conducted to explain behavioral responses for two rTMS target regions (M1 and aIPS), each comparing two connectivity modalities (static and dynamic). Importantly, counterparts of M1 and aIPS in the stroke-affected hemisphere did not show relevant overlap with stroke-lesions (supplementary Fig. S1). To examine whether results were stroke-specific, we repeated the regression analyses in healthy controls.

2.5.1. Input variables: Connectivity and data reduction

As input variables for the regression models, we used either dynamic or static connectivity. Based on the hypothesis that connectivity was related to regional contributions of M1 or aIPS, only connectivity values including the region of interest and its counterpart in the stroke-lesioned hemisphere were selected for each model.

Hence, all connectivity values involving either ipsi- or contralesional

M1 were selected as input variables when modeling M1 rTMS effects. Thus, the role of M1 was related to 37 static connectivity values (19 $M1_{ipsilesional}$ + 19 $M1_{contralesional}$ − 1 redundant M1 $_{ipsilesional}$ − M1 $_{contralesional}$), but 74 dynamic connectivity values (37 * 2 Connectivity States). Likewise, 37 static and 74 dynamic connectivity values involving ROIs in ipsi- or contralesional aIPS were selected for models on aIPS rTMS.

Input variables from static and dynamic connectivity were used for separate models to compare which best explained the roles of M1 and aIPS. Importantly, dynamic functional connectivity with two states includes twice as many connectivity states and thereby heavily increase the complexity of models based on dFNC, compared to static connectivity. To grant comparability of linear models with different numbers of input variables and to avoid problems resulting from multicollinearity, static as well as dynamic connectivity were reduced using principal component analyses (PCA) (Paul et al., 2021). Hence, for each region (M1 or aIPS), a 2D matrix of 37 static connectivity values * 18 stroke-affected individuals was entered into one PCA, while dFNC input (74 connectivity values * 18 stroke-affected individuals) was fed into a separate PCA. This allowed to condense the differently sized connectivity datasets into an equal amount of meaningful independent components. The Guttman-Kaiser criterion (Auerswald and Moshagen, 2019; Guttman, 1954) was applied to define which number of components from the PCA should be fed into the regression models, ensuring that only components capturing a substantial amount of variance of the data were included. Accordingly, for each region of interest, five principal components from static connectivity and five principal components from dFNC were derived, each serving as input variables for a separate linear regression model.

Of note, this approach was not designed to interpret single connections, but aims to optimize comparability between static and dynamic connectivity, minimizing multicollinearity and transforming the unequal numbers of connections between both modalities into comparable dimensions.

Yet, to understand which connections were most important determining each principal component, contributions were calculated by dividing the squared cosine of each connection by the sum of the squared cosines of all connections for a particular principal component. To illustrate which connectivity pattern mainly defined each principal component, contributions (in percent) higher than the average expected average contribution (100 % divided by all connections).

2.5.2. Outcome variable: The role of specific regions for movements

To quantify a region's role for hand movements, the Mean Movement Alteration was computed by normalizing the mean performance measures assessed during online-rTMS over the region relative to the performance during the control TMS condition (Hensel et al., 2023; Tscherpel et al., 2020b) (right panel, Fig. 1). Each of the three recorded movement types (finger tapping, pointing, grasping) was assessed regarding four kinematic features (efficiency, speed, smoothness, and accuracy), yielding twelve parameters in total (three tasks * four kinematic measures) (Hensel et al., 2023). To summarize the rTMS effects across these tasks and movement qualities, the percentage change of all twelve parameters during rTMS was averaged, serving as an outcome variable in the linear models.

3. Results

3.1. Sample

Stroke-affected individuals and healthy controls did not differ in age nor sex (Table 1, adopted from Hensel et al 2023). Stroke severity measured by the National Institutes of Health Stroke Scale (NIHSS) indicates that all patients showed moderate to severe deficits in the acute phase after stroke. A clinically relevant upper limb deficit within the first days after stroke was documented for all participants ranging from 1 (arm drifting) to 4 (no movement at all). Hence, we assumed that all patients underwent substantial motor system reorganization (Stinear et al., 2007; Ward, 2017).

3.2. No group differences in static functional connectivity

Static functional connectivity of individuals with stroke and healthy controls showed a high segregation of cortical, subcortical and cerebellar components (Fig. 2). ROIs of each network showed positive connectivity with regions of the same domain (e.g., between ROIs of the sensorimotor network), but weaker or negative connectivity with other domains (e.g. cortical sensorimotor and cerebellar ROIs). Comparing static connectivity of healthy participants, stroke-affected individuals with lower and those with higher motor outcome, one-way ANOVAs for each connectivity value did not show significant group differences after FDR-correction.

3.3. Dynamic functional connectivity

The analysis of dFNC identified two connectivity states (Fig. 3). The first state featured only weak connectivity between all ROIs. In contrast, the second state was characterized by a mostly positive connectivity between ROIs of the same network, while low or negative connectivity was observed between different networks. We refer to these states as low segregated (state 1) and highly segregated (state 2) states.

3.3.1. Performance-related temporal dynamics

Testing whether stroke − or different stroke outcomes – were linked to altered dynamic connectivity, a mixed ANOVA on *dwell time* detected an interaction between groups (healthy controls, individuals with higher and lower outcome after stroke) and brain states ($P < 0.001$; Fig. 3, Table 2). Correspondingly, the three level one way ANOVA for the symmetrical measure *fraction time* indicated significant between-group effects ($P < 0.001$). As indicated by dwell time, individuals with lower motor outcome after stroke spent more time in the highly segregated brain state 2 compared to healthy participants ($P = 0.001$) or individuals with higher outcome after stroke ($P = 0.002$), whereas healthy controls and individuals with higher motor outcome after stroke showed balanced dwell times between states. Likewise, the percentage of time spent in each state measured by fraction times showed that stroke-affected individuals with lower motor outcome spent 92.9 % of the time in the highly segregated state and only 7.1 % in the low segregated State 1. Again, fraction times did not show a predominant connectivity state for healthy participants and stroke-affected individuals with higher outcome. No significant between-group differences were found for the number of transitions, tested by a three level one way ANOVA ($P = 0.471$).

Corresponding to the subgroup differences, testing for correlations between all stroke-affected individuals' fraction time and the Motor Performance Score demonstrated that more time spent in the more segregated connectivity state 2 was associated with lower hand motor function (Pearson $r = -0.56$, $P = 0.014$, Fig. 3C). For state 1, fraction time showed an inverse correlation due to the symmetrical distribution of fraction times. Likewise, longer dwell times in state 2 correlated negatively with the Motor Performance Score (Pearson $r = -0.51$, $P = 0.030$), whereas longer dwell times in state 1 were positively correlated with performance (Pearson $r = 0.52$, $P = 0.026$). This relationship was inversely found at higher performance levels of individuals without stroke lesions (Fig. 3C). That is, healthy controls showed positive correlations between motor performance and fraction time (Pearson $r = 0.60$, $P = 0.008$) as well as dwell time in the more segregated brain state (Pearson $r = 0.58$, $P = 0.011$). In contrast, dwell times in the less segregated state 1 were negatively correlated with motor performance (Pearson $r = -0.63$, $P = 0.005$). In summary, more time spent in segregated dFNC is associated with more residual deficit after stroke, whereas segregation in the non-lesioned brain is associated with higher motor

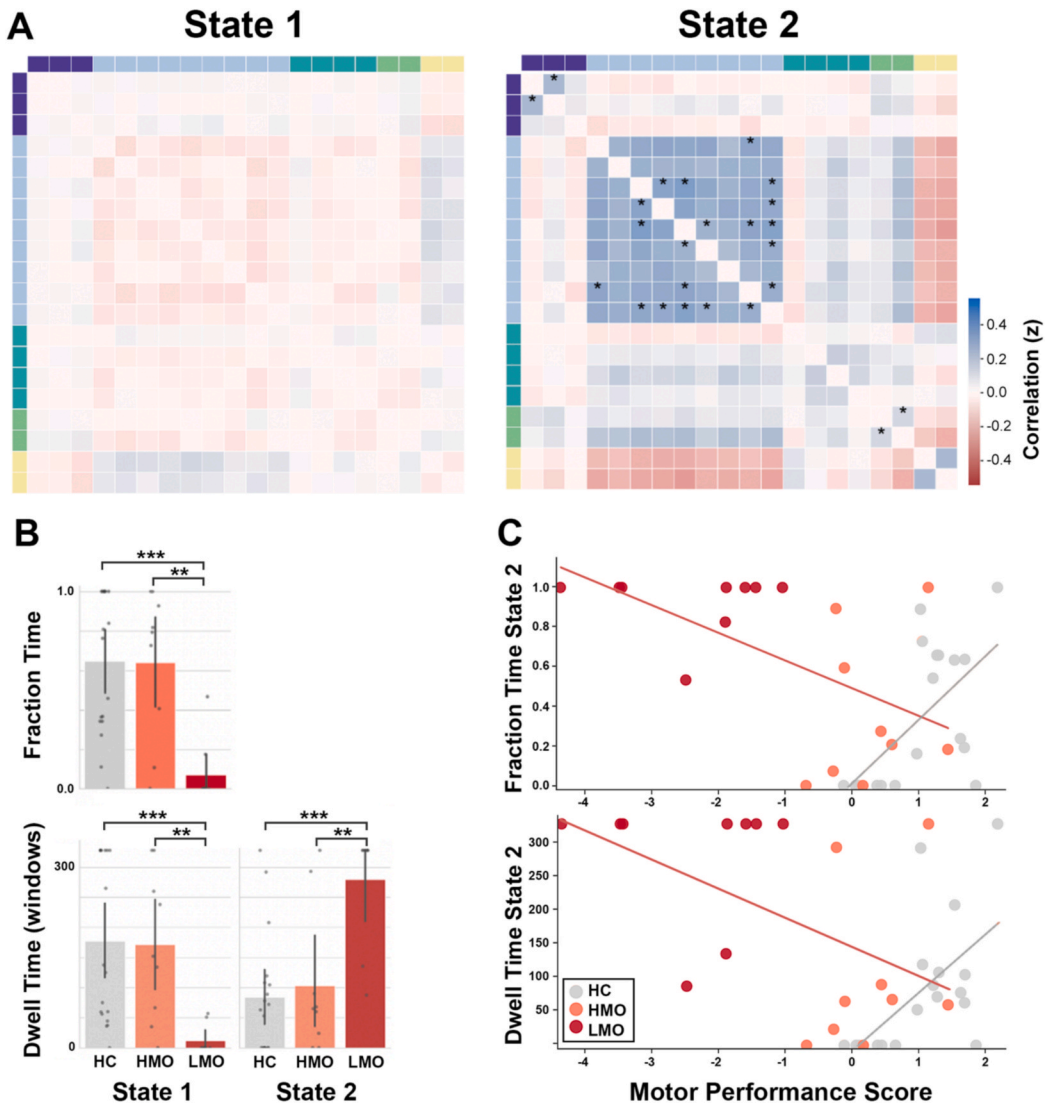

Fig. 3. Different dynamic connectivity in stroke (A) Distinguishing two connectivity states reveals stroke-related differences in state 2, indicated by asterisks (ANOVA $P < 0.05$, FDR-corrected). (B) Reduced mean fraction and dwell times in state 1 found in patients with lower outcome, compared to patients with higher outcome and healthy controls (between-group effect $P < 0.001$, asterisks indicate post hoc independent t-tests ***$P < 0.001$ **$P < 0.01$; HC = healthy controls, HMO = patients with higher motor outcome, LMO = patients with lower motor outcome). Fraction times were only compared for state1 due to their symmetry with state 2 (C) After stroke, low motor performance is associated with longer fraction (Pearson r = -0.56, P = 0.014) and dwell time (Pearson r = -0.51, P = 0.030). Separate regression lines for healthy controls illustrate that this relationship is inverted at higher levels of motor performance.

performance.

3.3.2. *Group differences in dynamic connectivity strength*

Individuals with lower outcome after stroke featured stronger connectivity between several ROIs of the sensorimotor and subcortical network, compared with healthy controls and patients with higher outcome (Supplementary Fig. S4). For example, increased connectivity was found between bilateral M1 as well as between the SMA and multiple precentral and paracentral regions, including bilateral M1 and the dorsal premotor cortex. No differences were found between individuals with higher outcome after stroke and healthy controls. In state 1, no differences were found at all. These findings correspond to observations in patients with more severe deficits in the acute phase after stroke, showing stronger dFNC between sensorimotor regions, specifically in the more segregated state (Bonkhoff et al., 2021b). Our findings suggest that – also in the chronic phase after stroke – motor deficits are linked to stronger dFNC predominantly between sensorimotor regions.

3.4. *Connectivity linked to motor-contributions of M1*

Backward regression models were used to estimate the relationship between connectivity involving bilateral M1 as input variables and the Mean Movement Alteration induced by rTMS over the contralesional M1, serving as an outcome variable. Since the comparison of models based on static and dynamic connectivity input variables was compromised by the different number of connectivity values in both modalities, PCA were first used to translate static and dFNC into an equal number of components. The Guttman-Kaiser criterion determined that including five principal components was sufficient to capture 80.7 % of the variance in all static and 74.5 % of the variance in all dynamic connections (across states 1 and 2). Thereby, we ensured an equal number of input variables (i.e., five) in both models, each reflecting distinct, minimally correlated patterns of connectivity (Fig. 4).

When computing regression models using stepwise backward elimination, the model using principal components derived from static connectivity could not significantly explain TMS effects (adjusted R^2 = 2.6 %). In contrast, the model using dFNC parameters (i.e. the second

Table 2
Brain state dynamics by group.

	Mean ± SD(Group 1)	Mean ± SD(Group 2)	Difference	df	T	P	Cohen's d
Dwell times State 1							
Healthy – Higher Outcome	177.3 ± 135.6	171.3 ± 123.5	6.0	25.0	0.11	0.912	0.05
Healthy – Lower Outcome	**177.3 ± 135.6**	**12.0 ± 23.9**	**165.3**	**25.0**	**3.60**	**0.001**	**1.47**
Higher – Lower Outcome	**171.3 ± 123.5**	**12.0 ± 23.9**	**159.3**	**16.0**	**3.80**	**0.002**	**1.79**
Dwell times State 2							
Healthy – Higher Outcome	84.2 ± 100.4	103.1 ± 121.9	−18.9	25.0	−0.43	0.670	−0.18
Healthy – Lower Outcome	**84.2 ± 100.4**	**279.9 ± 96.2**	**−195.7**	**25.0**	**−4.84**	**<0.001**	**−1.98**
Higher – Lower Outcome	**103.1 ± 121.9**	**279.9 ± 96.2**	**−176.8**	**16.0**	**−3.42**	**0.004**	**−1.61**
Fraction times State1							
Healthy – Higher Outcome	0.65 ± 0.36	0.64 ± 0.38	0.01	25.0	0.04	0.968	0.02
Healthy – Lower Outcome	**0.65 ± 0.36**	**0.07 ± 0.16**	**0.58**	**25.0**	**4.58**	**<0.001**	**1.87**
Higher – Lower Outcome	**0.64 ± 0.38**	**0.07 ± 0.16**	**0.57**	**16.0**	**4.16**	**0.001**	**1.96**
Number of Transitions							
Healthy – Higher Outcome	1.39 ± 1.50	1.22 ± 1.30					
Healthy – Lower Outcome	1.39 ± 1.50	0.67 ± 1.41					
Higher – Lower Outcome	1.22 ± 1.30	0.67 ± 1.41					

Results of post hoc independent t-tests after significant interaction ($P < 0.001$) in the repeated measures ANOVA for dwell times and the significant one way ANOVA for fraction time ($P < 0.001$). Fraction times were only compared for state1 and not state 2 due to their symmetry (see Methods). The one way ANOVA for the number of transitions was not significant ($P = 0.471$). SD = standard deviation. df = degrees of freedom. Significant results in bold.

principal component) significantly explained the TMS effect evoked upon contralesional M1 stimulation, yielding 26.6 % of the explained variance ($p = 0.029$, adjusted $R^2 = 22.0$ %, BIC = 28.9), as described in the following equation:

$$\text{TMS-Effect}_{cM1} = -0.3 * PC2_{dynamic}$$

Consequently, dynamic but not static connectivity was associated with the role of contralesional M1 in post-stroke hand movements (Fig. 4).

In the healthy group, the Kaiser-Guttman criterion suggested retaining seven components for dynamic connectivity and five for static connectivity. To ensure comparability between dynamic and static connectivity as well as between cohorts (patients and healthy controls), we limited the number of components to five in all analyses. As a result, the regression models for healthy participants captured 74.3 % of the variance in static connectivity and 64.1 % in dynamic connectivity. Regression analysis using these five components revealed that both dynamic and static connectivity were associated with individual variability in TMS effects over contralesional M1 in healthy controls. The dynamic connectivity model yielded 24.3 % of the explained variance ($p = 0.038$, adjusted $R^2 = 19.6$ %, BIC = 38.7), as described in the equation:

$$\text{TMS-Effect}_{cM1\ (healthy)} = 0.6 * PC5_{dynamic\ (healthy)}$$

Similarly, the static connectivity model yielded 32.2 % explained variance ($p = 0.014$, adjusted $R^2 = 27.9$ %, BIC = 44.6).

$$\textit{TMS-Effect}_{cM1\ (healthy)} = 0.4 * PC4_{static\ (healthy)}.$$

3.5. Connectivity linked to motor-contributions of aIPS

Like for M1, PCA-informed stepwise backward regression models were computed based on connectivity involving bilateral aIPS as input variables and the Mean Movement Alteration by rTMS over the aIPS as an outcome variable. For aIPS, PCA derived input variables accounted for 74.7 % of the variance of static connections and 73.6 % of the variance of dynamic connections. Models featured significant results with both input from static and dynamic connectivity. The regression model informed by static connectivity explained 33.8 % of variance of rTMS effects ($p = 0.011$, adjusted $R^2 = 29.6$ %, BIC = 39.0), with the equation:

$$\text{TMS-Effect}_{caIPS} = 1.1 * PC5_{static}$$

The regression model based on dynamic connectivity explained 33.7 % of variance of rTMS effects ($p = 0.012$, adjusted $R^2 = 29.5$ %, BIC = 39.0), based on the equation:

$$\text{TMS-Effect}_{caIPS} = 0.6 * PC3_{dynamic}$$

Notably, both components selected by linear models, namely PC5 for static and PC3 for dynamic connectivity reflect connectivity with basal ganglia, cerebellum and cortical sensorimotor regions (Fig. 5). In sum, both static and dynamic connectivity explained the role of the contralesional aIPS for hand movements to a very similar degree.

For healthy participants, regression models did not yield significant associations for either dynamic or static connectivity, suggesting that TMS-induced effects over aIPS were not robustly explained by functional connectivity in this group.

3.6. Replication analysis

To ensure comparability with earlier studies using dynamic functional connectivity in stroke (Bonkhoff et al., 2021, 2020) we primarily used an ICA template derived from a stroke-relevant dataset (Allen et al., 2014). This choice allowed direct comparison with previously published findings. However, to evaluate the robustness of our results, we repeated the PCA-based dimensionality reduction and backward linear regression models using two recent, large-scale ICA templates: (1) Neuromark_fMRI_2.2 based on over 100,000 individuals (Iraji et al., 2023; Jensen et al., 2024), and (2) Neuromark_fMRI_3.0_aging, which includes participants more representative of our sample's age range (Fu et al., 2024). As shown in the supplementary material (Table S1), the

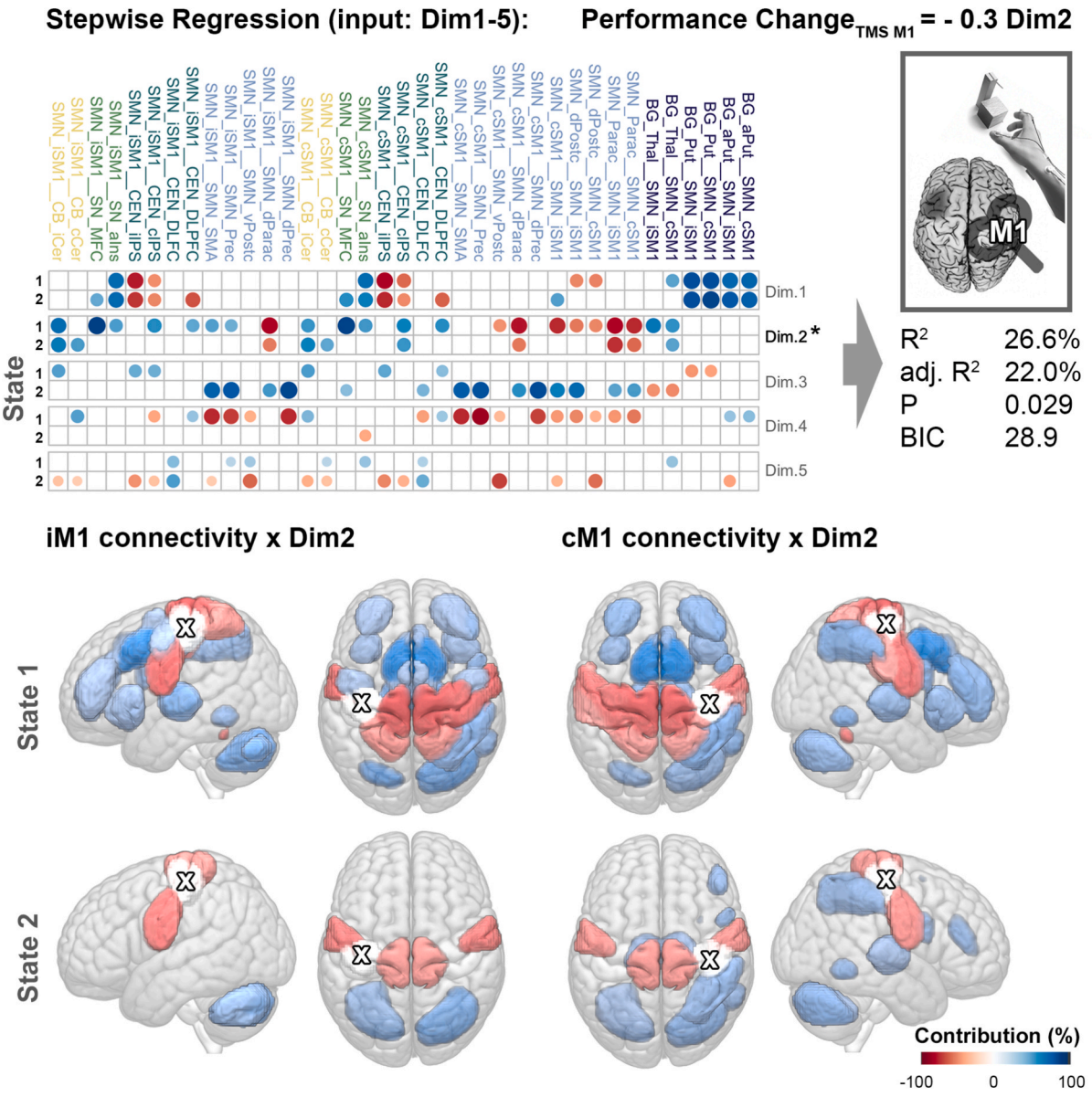

Fig. 4. Connectivity linked to rTMS effects on contralesional M1. (Top) Patients' role of contralesional M1 could be explained by dynamic but not static connectivity. Matrices indicate contributions of each connectivity (columns) to each PCA-dimension (rows). Dimension 2 was selected by the stepward regression model to explain the effects of contralesional rTMS, with a negative weight of −0.3. Note that, compared to the other dimensions, Dimension 2 receives most contributions from connections within the sensorimotor system and cerebellum. (Bottom) Connectivity reflected by Dimension 2, involving a varying connectivity of a widely connected pattern between M1 and all subnetworks in state 1, and a more restricted pattern including mainly sensorimotor and cerebellar connections in state 2. cM1 = contralesional M1, iM1 = ipsilesional M1.

relationship of specifically dynamic connectivity (not static connectivity) with TMS effects over M1 can be consistently shown. (for more details see supplementary material).

4. Discussion

We here compared static and dynamic functional connectivity with respect to TMS-induced motor changes in chronic stroke patients. In line with previous research in individuals with stroke (Bonkhoff et al., 2020a; Hu et al., 2018), dFNC revealed transient connectivity states which differed in network segregation, indicating that individuals with a less favorable outcome spend more time in a more segregated state. Linking this finding to the effects on hand movements, induced by online-rTMS after the fMRI session, regression models indicated that dFNC was associated with the contributions of both contralesional M1 and aIPS for motor performance, whereas the classic static connectivity was merely indicative of rTMS-effects for the contralesional aIPS. In summary, our findings suggest that contralesional regions' dynamic connectivity shifts between more and less segregated brain states reflect behaviorally meaningful information for hand motor performance after stroke.

4.1. Dynamic connectivity related to stroke-impairment

The present study links lower motor outcome in the chronic phase after stroke with longer occupancy of connectivity state 2, featuring a high level of network segregation (Fig. 3C). This association was demonstrated by group differences, showing that individuals with lower motor outcome spent more time in state 2, and by a linear relationship between low motor performance after stroke and the occupancy of state 2. This observation is in line with dynamic connectivity studies in acute patients, finding higher segregation of networks (Bonkhoff et al., 2020a,

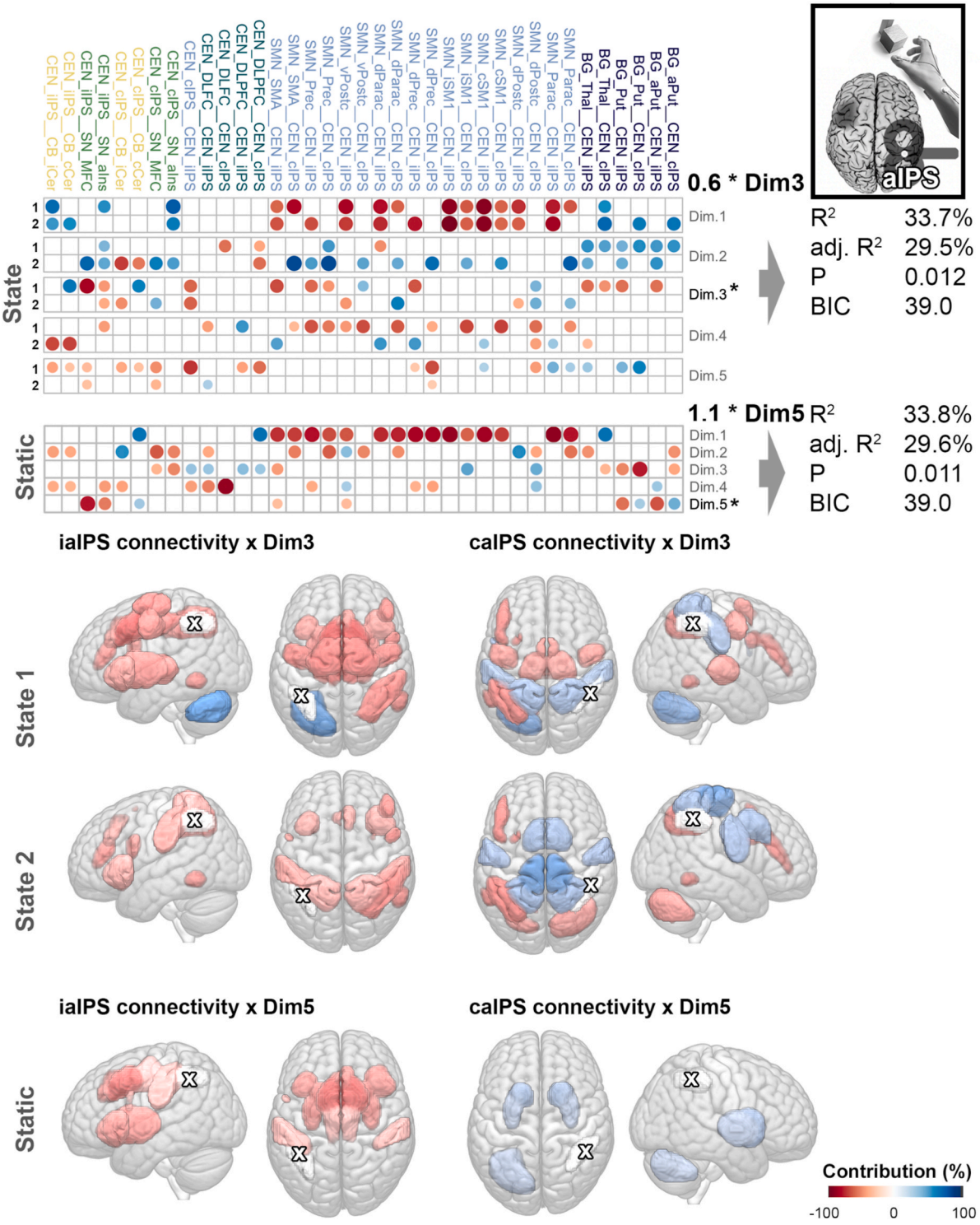

Fig. 5. Connectivity linked to rTMS effects on contralesional aIPS. (Top) Patients' role of contralesional aIPS was explained by dynamic and static. Matrices indicate contributions of each connectivity (columns) to each PCA-dimensions (rows). Dimensions selected in each model (3 and 5, respectively) were both positively weighted for rTMS effects. Compared to the other dimensions, dynamic dimension 3 and static dimension 5 are both driven by the connection between ipsilesional aIPS and the medial frontal cortex and putamen (Bottom) Anatomical visualization of connectivity patterns reflected by Dimensions 3 (dynamic connectivity) and 5 (static connectivity). caIPS = contralesional aIPS, iaIPS = ipsilesional aIPS.

2021b), and reduced temporal variability (Hu et al., 2018) early after stroke, both discussed to reflect deficits in network integration. Towards the chronic phase, a normalization of this pattern was associated with motor recovery (Hu et al., 2018). Stroke lesions have been suggested to disrupt the successful integration of information across domains, which likely relies on shifting between more integrative or segregative states (Deco et al., 2015; Duncan and Small, 2018; Eickhoff and Grefkes, 2011). Compared to previous findings from the acute phase, the present findings from the chronic phase after stroke show a pattern of segregation, with negative connectivity between the sensorimotor network and visual, cerebellar, and subcortical networks (Bonkhoff 2021, Bonkhoff 2020). It should be noted that other networks in these brain states were

more integrated, such as the frontoparietal and the default mode network, similar to the positive correlation observed between frontoparietal regions in state 2 of the present work. We, therefore, stress that network segregation in our work specifically refers to the relative isolation of the sensorimotor network, for example from cerebellar and subcortical regions. Bonkhoff et al. (2021) further found that severely affected patients with acute stroke spent more time in such a connectivity state, indicating that dFNC recorded at rest relates to post-stroke behavior. It should be noted, however, that stroke severity in the work of Bonkhoff et al (2021) was determined by the NIHSS, a clinical score summarizing a wide range of deficits including sensory, motor, language and visuospatial function, whereas the present analysis focused on analyzing hand movements in higher precision. Thus, by differentiating patient subgroups by motor outcome, we demonstrate that a higher segregation of the sensorimotor network may sustain towards the chronic phase in individuals with residual upper limb deficits. This is in line with the analysis of dFNC in longitudinal data suggesting that the initially observed abnormalities of dFNC may return to normal levels depending on clinical recovery (Bonkhoff et al., 2021b; Duncan and Small, 2018; Favaretto et al., 2022). In line with this notion, longitudinal data from individuals with traumatic brain injury suggest an early decrease of segregation in individuals with more successful recovery (Kuceyeski et al., 2019). Hence, the perseverance in highly-segregated brain states evolves as a signature of less successful recovery, reflecting unsuccessful or maybe even maladaptive reorganization.

In line with this notion, individuals with lower motor outcome showed pronounced connectivity strength of intra-domain connections in the sensorimotor, salience and basal ganglia networks (Fig. 3, Supplementary Fig. S4). Besides sensorimotor and subcortical regions, the fronto-insular connections of the salience network might therefore play a critical role for long-term motor outcome. Enhanced connectivity between the bilateral insulae and medial frontal cortex were previously linked to cognitive dysfunction in the subacute and chronic phase after stroke (Vicentini et al., 2021). Additionally, altered temporal variability of the insula (Hu et al., 2018) and enhanced connectivity between the contralesional insula and the ipsilesional M1 (Chen et al., 2018) have been previously found in acute patients with motor deficits. Both studies have assessed motor deficits by the Fugl-Meyer assessment, whereas the present findings add evidence from kinematic analyses of hand function. While the upper limb score of the Fugl-Meyer mainly captures body function such as the range of motion, reflex activity and coordination (Fugl-Meyer et al., 1975), kinematic data provide a more sensitive readout of motor control such as smoothness and accuracy as well as motor execution by movement efficiency and speed. Moreover, kinematic recordings were only conducted in distal upper limb movements, which involve more dexterous movements, without some of the gross movements involving shoulder and core as measured by the Fugl-Meyer assessment. In sum, the present study extends previous findings linking increased dynamic connectivity between cortical and subcortical sensorimotor regions and the saliency network with impaired motor control and execution of distal hand movements.

4.2. Insights from online-rTMS interference

To this end, the neural neurophysiology underlying a more segregated connectivity in individuals with stroke-induced hemiparesis remained largely speculative. Using online-rTMS after the fMRI session allowed to transiently disrupt neural processing in the contralesional M1 and aIPS during hand movements, suggesting that time-variant dFNC provides information on the roles of the contralesional M1 and aIPS for motor function. Hence, shifts between integrated and segregated connectivity states as identified by dFNC may reflect processes related to motor-contributions of brain regions involved in such connectivity patterns. Possibly related to the prolonged connectivity state with high interconnectivity between sensorimotor regions at rest, extensive activation of bilateral sensorimotor regions during motor tasks has been discussed to reflect different mechanisms in healthy ageing and stroke (Tscherpel et al., 2020a; Ward et al., 2003). While this activation pattern has been similarly found in older individuals without lesions as well as with stroke, rTMS studies helped to differentiate such abnormally high activations between healthy ageing and individuals with acute as well as chronic stroke (Lotze et al., 2006; Tscherpel et al., 2020b; Volz et al., 2017). For example, Volz and colleagues (2017) have shown that patients with acute stroke perform faster finger tapping with their stroke affected hand when neural processing is disrupted during rTMS applied to contralesional M1, indicating a maladaptive role of this region early after stroke. In contrast, applying rTMS in individuals in the chronic phase after stroke deteriorated motor performance when targeting contralesional M1 (Lotze et al., 2006) and the dorsal premotor cortex (Lotze et al., 2006; Tscherpel et al., 2020b). Broadly, two competing mechanisms have been proposed regarding the reorganization of neural networks after a brain lesion. One concept known as the vicariation theory suggests that intact brain regions establish new connections to compensate for dysfunctional network components after stroke (Finger, 2009; Wiesendanger, 2006). On the other hand, altered connectivity may arise from dysfunctional, possibly competitive mechanisms originating in under-regulated brain regions after stroke. While both concepts may explain altered connectivity, the first would arise from neural mechanisms supporting recovered function whereas the other may be a marker of aberrant processing, often referred to as maladaptation (Hinder, 2012; Hummel and Cohen, 2006; Murase et al., 2004; Nowak et al., 2009). The present study links the effects induced by rTMS with dynamic connectivity using stepwise linear regression models. The connectivity pattern associated with rTMS effects for both contralesional M1 and aIPS involved dFNC with sensorimotor cortical regions, basal ganglia and the cerebellum (Figs. 4 and 5). Together, these findings indicate that time-varying connectivity states contain information on the behavioral implications of different nodes of the motor system. Regarding some regions, in our case M1, such information could not be detected by static connectivity. In other words, the influence of the contralesional M1 is related to network dynamics, rather than connectivity patterns which are stable over time. To test whether these findings are specific to the stroke lesion, regression analyses were comparably conducted in healthy participants. Interestingly, both static and dynamic connectivity explained a substantial portion of variance in TMS effects when stimulating contralesional M1, but no associations were found for aIPS. These findings support the notion that, also in the absence of stroke-related reorganization, hand motor performance involves signaling between bilateral M1 (Perez and Cohen, 2008; Rehme et al., 2013). In contrast, dynamic connectivity with contralesional aIPS may be more relevant for hand movements after stroke. In summary, we extend previous reports suggesting that dynamic connectivity provides higher sensitivity discriminating time-sensitive features of neural processing in health and disease, including perceptual cues in healthy individuals (Di et al., 2022), and detecting clinically relevant connectivity alterations in stroke (Bonkhoff et al., 2020b) as well as other pathologies (Jin et al., 2017; Madhyastha et al., 2015). Thereby, assessing dynamic connectivity may be a promising extension of current markers aiding the personalized application of neuromodulation after stroke.

4.3. Limitations

Some limitations should be considered. First, the complex experimental setup including fMRI and subsequent online-rTMS, which requires multiple repetitions of complex upper limb movements excluded severely affected stroke patients. While all patients showed moderate or severe deficits in the acute phase, they were only mildly or moderately affected during the online TMS session of our study. Although the sample of 18 stroke-affected participants and 18 healthy controls exceeds that of many earlier online-rTMS stroke studies, it remains insufficient for broadly generalizing the findings. Second, although detailed kinematic measurements allow a sensitive assessment of motor

performance changes under rTMS, other individual factors, such as hand dominance or general motor learning ability, may also contribute to task performance. These factors should be considered in future studies aiming to explain network contributions linked to motor outcome after stroke. Third, although all participants were studied in the chronic post-stroke phase, heterogeneity in lesion location and individual recovery trajectories could have introduced additional variability into the connectivity measures. Fourth, the cross-sectional design does not allow us to infer whether the observed dynamic connectivity patterns remain stable or evolve further over time. Finally, while we used resting-state fMRI to characterize network organization, combining resting and task-based measurements in future studies may provide more comprehensive insights into how dynamic connectivity relates to motor performance during stroke recovery.

5. Conclusion

The present work compared dynamic and static functional connectivity in chronic stroke and healthy controls, extending previous evidence that transient states of highly segregated networks related to motor control and execution are linked to worse motor outcome. Importantly, the present study indicates distinct mechanisms of such segregation with regards to physiological motor function and stroke-related impairment. Finally, dynamic functional connectivity was demonstrated to contain movement-related information on contralesional M1 and aIPS, whereas static connectivity could only explain rTMS effects induced in the contralesional aIPS. Together with recent dynamic functional connectivity studies in individuals with stroke, our findings highlight that analyzing transient shifts between brain states unveil outcome-dependent network configurations. Moreover, this is the first study providing proof of concept that dynamic functional connectivity relates to behavioral responses induced by rTMS, which helped to infer the roles of motor-related brain regions for motor recovery.

CRediT authorship contribution statement

Lukas Hensel: Writing – review & editing, Writing – original draft, Visualization, Validation, Software, Methodology, Investigation, Formal analysis, Data curation, Conceptualization. **Anna K. Bonkhoff:** Writing – review & editing, Validation, Software, Formal analysis. **Theresa Paul:** Writing – review & editing, Software, Methodology, Formal analysis. **Caroline Tscherpel:** Writing – review & editing, Methodology, Investigation, Data curation, Conceptualization. **Fabian Lange:** Writing – review & editing, Investigation, Data curation, Conceptualization. **Shivakumar Viswanathan:** Writing – review & editing, Visualization, Software, Methodology, Formal analysis. **Lukas J. Volz:** Writing – review & editing, Software, Methodology. **Simon B. Eickhoff:** Writing – review & editing, Formal analysis. **Gereon R. Fink:** Writing – review & editing, Supervision, Resources, Funding acquisition. **Christian Grefkes:** Writing – review & editing, Validation, Supervision, Resources, Project administration, Methodology, Investigation, Funding acquisition, Conceptualization.

Funding

CG, CT, LJV, SBE and GRF are funded by the Deutsche Forschungsgemeinschaft (DFG, German Research Foundation) – Project-ID 431,549,029 – SFB 1451 (projects B05, B06, C05 and Z03).

Declaration of Competing Interest

The authors declare that they have no known competing financial interests or personal relationships that could have appeared to influence the work reported in this paper.

Appendix A. Supplementary data

Supplementary data to this article can be found online at https://doi.org/10.1016/j.nicl.2025.103825.

Data availability

The functions used to compute static connectivity and dFNC are publicly available in the GIFT toolbox. The kinematic data during real and control TMS conditions, the ensuing rTMS effects, as well as behavioral scores of each participant have been published at https://github.com/LukasHensel/chronic_stroke_fc_tms. Components used for the constrained ICA are available at http://trendscenter.org/software.

References

Allen, E.A., Damaraju, E., Plis, S.M., Erhardt, E.B., Eichele, T., Calhoun, V.D., 2014. Tracking whole-brain connectivity dynamics in the resting state. Cereb. Cortex 24, 663–676. https://doi.org/10.1093/cercor/bhs352.

Ashburner, J., Friston, K.J., 2005. Unified segmentation. Neuroimage 26, 839–851. https://doi.org/10.1016/j.neuroimage.2005.02.018.

Auerswald, M., Moshagen, M., 2019. How to determine the number of factors to retain in exploratory factor analysis: a comparison of extraction methods under realistic conditions. Psychol. Methods 24, 468–491. https://doi.org/10.1037/met0000200.

Baldassarre, A., Ramsey, L., Siegel, J.S., Shulman, G.L., Corbetta, M., 2016. Brain connectivity and neurological disorders after stroke. Curr. Opin. Neurol. 29, 706–713.

Binkofski, F., Buccino, G., Posse, S., Seitz, R.J., Rizzolatti, G., Freund, H., 1999. A fronto-parietal circuit for object manipulation in man: evidence from an fMRI-study. Eur. J. Neurosci. 11, 3276–3286. https://doi.org/10.1046/j.1460-9568.1999.00753.x.

Bonkhoff, A.K., Espinoza, F.A., Gazula, H., Vergara, V.M., Hensel, L., Michely, J., Paul, T., Rehme, A.K., Volz, L.J., Fink, G.R., Calhoun, V.D., Grefkes, C., 2020a. Acute ischaemic stroke alters the brain's preference for distinct dynamic connectivity states. Brain 143, 1525–1540. https://doi.org/10.1093/brain/awaa101.

Bonkhoff, A.K., Grefkes, C., 2022. Precision medicine in stroke: towards personalized outcome predictions using artificial intelligence. Brain J. Neurol. 145, 457–475. https://doi.org/10.1093/brain/awab439.

Bonkhoff, A.K., Rehme, A.K., Hensel, L., Tscherpel, C., Volz, L.J., Espinoza, F.A., Gazula, H., Vergara, V.M., Fink, G.R., Calhoun, V.D., Rost, N.S., Grefkes, C., 2021a. Dynamic connectivity predicts acute motor impairment and recovery post-stroke. Brain Commun. 3, fcab227. https://doi.org/10.1093/braincomms/fcab227.

Bonkhoff, A.K., Schirmer, M.D., Bretzner, M., Etherton, M., Donahue, K., Tuozzo, C., Nardin, M., Giese, A., Wu, O., Calhoun, V.D., Grefkes, C., Rost, N.S., 2021b. Abnormal dynamic functional connectivity is linked to recovery after acute ischemic stroke. Hum. Brain Mapp. 42, 2278–2291. https://doi.org/10.1002/hbm.25366.

Bonkhoff, A.K., Schirmer, M.D., Bretzner, M., Hong, S., Regenhardt, R.W., Brudfors, M., Donahue, K.L., Nardin, M.J., Dalca, A.V., Giese, A.-K., Etherton, M.R., Hancock, B.L., Mocking, S.J.T., McIntosh, E.C., Attia, J., Benavente, O.R., Bevan, S., Cole, J.W., Donatti, A., Griessenauer, C.J., Heitsch, L., Holmegaard, L., Jood, K., Jimenez-Conde, J., Kittner, S.J., Lemmens, R., Levi, C.R., McDonough, C.W., Meschia, J.F., Phuah, C.-L., Rolfs, A., Ropele, S., Rosand, J., Roquer, J., Rundek, T., Sacco, R.L., Schmidt, R., Sharma, P., Slowik, A., Söderholm, M., Sousa, A., Stanne, T.M., Strbian, D., Tatlisumak, T., Thijs, V., Vagal, A., Wasselius, J., Woo, D., Zand, R., McArdle, P. F., Worrall, B.B., Jern, C., Lindgren, A.G., Maguire, J., Bzdok, D., Wu, O., Consortium, M.-G. and G.I. and the I.S.G., Rost, N.S., 2020b. Outcome after acute ischemic stroke is linked to sex-specific lesion patterns. Nat. Commun. 12, 3289. Doi: 10.1038/s41467-021-23492-3.

Calhoun, V.D., Adali, T., Pearlson, G.D., Pekar, J.J., 2001. A method for making group inferences from functional MRI data using independent component analysis. Hum. Brain Mapp. 14, 140–151. https://doi.org/10.1002/hbm.1048.

Calhoun, V.D., Miller, R., Pearlson, G., Adalı, T., 2014. The Chronnectome: Time-Varying Connectivity Networks as the Next Frontier in fMRI Data Discovery. Neuron 84, 262–274. https://doi.org/10.1016/j.neuron.2014.10.015.

Carter, A.R., Astafiev, S.V., Lang, C.E., Connor, L.T., Rengachary, J., Strube, M.J., Pope, D.L.W., Shulman, G.L., Corbetta, M., 2010. Resting interhemispheric functional magnetic resonance imaging connectivity predicts performance after stroke. Ann. Neurol. 67, 365–375. https://doi.org/10.1002/ana.21905.

Caspers, S., Amunts, K., Zilles, K., 2012. Posterior parietal cortex: multimodal association cortex. the Human nervous System 1036–1055. doi: 10.1016/b978-0-12-374236-0.10028-8 Chang, C., Glover, G.H., 2010. Time–frequency dynamics of resting-state brain connectivity measured with fMRI. Neuroimage 50, 81–98. https://doi.org/10.1016/j.neuroimage.2009.12.011.

Chang, C., Glover, G.H., 2010. Time–frequency dynamics of resting-state brain connectivity measured with fMRI. Neuroimage 50, 81–98. https://doi.org/10.1016/j.neuroimage.2009.12.011.

Chen, J., Sun, D., Shi, Y., Jin, W., Wang, Y., Xi, Q., Ren, C., 2018. Alterations of static functional connectivity and dynamic functional connectivity in motor execution regions after stroke. Neurosci. Lett. 686, 112–121. https://doi.org/10.1016/j.neulet.2018.09.008.

Cox, R.W., 1996. AFNI: Software for Analysis and Visualization of Functional magnetic Resonance Neuroimages. Comput. Biomed. Res. 29, 162–173. https://doi.org/10.1006/cbmr.1996.0014.
Culham, J.C., Valyear, K.F., 2006. Human parietal cortex in action. Current Opinion in Neurobiology 16, 205–212. https://doi.org/10.1016/j.conb.2006.03.005.
Damaraju, E., Allen, E.A., Belger, A., Ford, J.M., McEwen, S., Mathalon, D.H., Mueller, B. A., Pearlson, G.D., Potkin, S.G., Preda, A., Turner, J.A., Vaidya, J.G., van Erp, T.G., Calhoun, V.D., 2014. Dynamic functional connectivity analysis reveals transient states of dysconnectivity in schizophrenia. Neuroimage Clin. 5, 298–308. https://doi.org/10.1016/j.nicl.2014.07.003.
Davare, M., Kraskov, A., Rothwell, J.C., Lemon, R.N., 2011. Interactions between areas of the cortical grasping network. Curr. Opin. Neurobiol. 21, 565–570. https://doi.org/10.1016/j.conb.2011.05.021.
Deco, G., Tononi, G., Boly, M., Kringelbach, M.L., 2015. Rethinking segregation and integration: contributions of whole-brain modelling. Nat. Rev. Neurosci. 16, 430–439. https://doi.org/10.1038/nrn3963.
Di, X., Zhang, Z., Xu, T., Biswal, B.B., 2022. Dynamic and stationary brain connectivity during movie watching as revealed by functional MRI. Brain Struct. Funct. 1–14. https://doi.org/10.1007/s00429-022-02522-w.
Díez-Cirarda, M., Strafella, A.P., Kim, J., Peña, J., Ojeda, N., Cabrera-Zubizarreta, A., Ibarretxe-Bilbao, N., 2018. Dynamic functional connectivity in Parkinson's disease patients with mild cognitive impairment and normal cognition. Neuroimage Clin. 17, 847–855. https://doi.org/10.1016/j.nicl.2017.12.013.
Du, Y., Allen, E.A., He, H., Sui, J., Wu, L., Calhoun, V.D., 2016. Artifact removal in the context of group ICA: a comparison of single-subject and group approaches. Hum. Brain Mapp. 37, 1005–1025. https://doi.org/10.1002/hbm.23086.
Du, Y., Fan, Y., 2013. Group information guided ICA for fMRI data analysis. Neuroimage 69, 157–197. https://doi.org/10.1016/j.neuroimage.2012.11.008.
Duncan, E.S., Small, S.L., 2018. Changes in dynamic resting state network connectivity following aphasia therapy. Brain Imaging Behav. 12, 1141–1149. https://doi.org/10.1007/s11682-017-9771-2.
Eickhoff, S.B., Grefkes, C., 2011. Approaches for the integrated analysis of structure, function and connectivity of the human brain. Clin. EEG Neurosci. 42, 107–121. https://doi.org/10.1177/155005941104200211.
Espinoza, F.A., Turner, J.A., Vergara, V.M., Miller, R.L., Mennigen, E., Liu, J., Misiura, M. B., Ciarochi, J., Johnson, H.J., Long, J.D., Bockholt, H.J., Magnotta, V.A., Paulsen, J. S., Calhoun, V.D., 2018. Whole-Brain Connectivity in a Large Study of Huntington's Disease Gene Mutation Carriers and healthy Controls. Brain Connect. 8, 166–178. https://doi.org/10.1089/brain.2017.0538.
Favaretto, C., Allegra, M., Deco, G., Metcalf, N.V., Griffis, J.C., Shulman, G.L., Brovelli, A., Corbetta, M., 2022. Subcortical-cortical dynamical states of the human brain and their breakdown in stroke. Nat. Commun. 13, 5069. https://doi.org/10.1038/s41467-022-32304-1.
Finger, S., 2009. Recovery of function: Redundancy and vicariation theories. Handb. Clin. Neurol. 95, 833–841. https://doi.org/10.1016/s0072-9752(08)02151-9.
Finger, S., Koehler, P.J., Jagella, C., 2004. The monakow concept of diaschisis: origins and perspectives. Arch Neurol-Chicago 61, 283–288. https://doi.org/10.1001/archneur.61.2.283.
Fiorenzato, E., Strafella, A.P., Kim, J., Schifano, R., Weis, L., Antonini, A., Biundo, R., 2019. Dynamic functional connectivity changes associated with dementia in Parkinson's disease. Brain 142, 2860–2872. https://doi.org/10.1093/brain/awz192.
Fu, Z., Batta, I., Wu, L., Abrol, A., Agcaoglu, O., Salman, M.S., Du, Y., Iraji, A., Shultz, S., Sui, J., Calhoun, V.D., 2024. Searching reproducible brain features using neuromark: templates for different age populations and imaging modalities. Neuroimage 292, 120617. https://doi.org/10.1016/j.neuroimage.2024.120617.
Fugl-Meyer, A.R., Jääskö, L., Leyman, I., Olsson, S., Steglind, S., 1975. The post-stroke hemiplegic patient. a method for evaluation of physical performance. Scand. J. Rehabil. Med. 7, 13–31.
Golestani, A.-M., Tymchuk, S., Demchuk, A., Goodyear, B.G., Group, V.-2 S., 2013. Longitudinal evaluation of resting-state FMRI after acute stroke with hemiparesis. Neurorehabilitation and neural repair 27, 153–163. Doi: 10.1177/1545968312457827.
Grefkes, C., Fink, G.R., 2016. Noninvasive brain stimulation after stroke: it is time for large randomized controlled trials! Curr. Opin. Neurol. 29, 714–720. https://doi.org/10.1097/wco.0000000000000395.
Grefkes, C., Fink, G.R., 2014. Connectivity-based approaches in stroke and recovery of function. Lancet Neurol. 13, 206–216. https://doi.org/10.1016/s1474-4422(13)70264-3.
Grefkes, C., Fink, G.R., 2005. The functional organization of the intraparietal sulcus in humans and monkeys. J. Anat. 207, 3–17. https://doi.org/10.1111/j.1469-7580.2005.00426.x.
Grefkes, C., Nowak, D.A., Wang, L.E., Dafotakis, M., Eickhoff, S.B., Fink, G.R., 2010. Modulating cortical connectivity in stroke patients by rTMS assessed with fMRI and dynamic causal modeling. Neuroimage 50, 233–242. https://doi.org/10.1016/j.neuroimage.2009.12.029.
Guttman, L., 1954. Some necessary conditions for common-factor analysis. Psychometrika 19, 149–161. https://doi.org/10.1007/bf02289162.
Hensel, L., Lange, F., Tscherpel, C., Viswanathan, S., Freytag, J., Volz, L.J., Eickhoff, S.B., Fink, G.R., Grefkes, C., 2023. Recovered grasping performance after stroke depends on interhemispheric frontoparietal connectivity. Brain 146, 1006–1020. https://doi.org/10.1093/brain/awac157.
Hensel, L., Tscherpel, C., Freytag, J., Ritter, S., Rehme, A.K., Volz, L.J., Eickhoff, S.B., Fink, G.R., Grefkes, C., 2021. Connectivity-Related Roles of Contralesional Brain Regions for Motor Performance Early after Stroke. Cereb. Cortex 31, 993–1007. https://doi.org/10.1093/cercor/bhaa270.
Hinder, M.R., 2012. Interhemispheric connectivity between distinct motor regions as a window into bimanual coordination. J. Neurophysiol. 107, 1791–1794. https://doi.org/10.1152/jn.00822.2011.
Hoffstaedter, F., Grefkes, C., Zilles, K., Eickhoff, S.B., 2013. The "what" and "when" of Self-Initiated Movements. Cereb. Cortex 23, 520–530. https://doi.org/10.1093/cercor/bhr391.
Hu, J., Du, J., Xu, Q., Yang, F., Zeng, F., Weng, Y., Dai, X., Qi, R., Liu, X., Lu, G., Zhang, Z., 2018. Dynamic network analysis reveals altered temporal variability in brain regions after stroke: a longitudinal resting-state fMRI study. Neural Plast. 2018, 9394156. https://doi.org/10.1155/2018/9394156.
Hummel, F.C., Cohen, L.G., 2006. Non-invasive brain stimulation: a new strategy to improve neurorehabilitation after stroke? Lancet Neurol. 5, 708–712. https://doi.org/10.1016/s1474-4422(06)70525-7.
Jin, C., Jia, H., Lanka, P., Rangaprakash, D., Li, L., Liu, T., Hu, X., Deshpande, G., 2017. Dynamic brain connectivity is a better predictor of PTSD than static connectivity. Hum. Brain Mapp. 38, 4479–4496. https://doi.org/10.1002/hbm.23676.
Kessner, S.S., Schlemm, E., Cheng, B., Bingel, U., Fiehler, J., Gerloff, C., Thomalla, G., 2019. Somatosensory Deficits after Ischemic Stroke. Stroke 50, 1116–1123. https://doi.org/10.1161/strokeaha.118.023750.
Koch, P.J., Hummel, F.C., 2017. Toward precision medicine: tailoring interventional strategies based on noninvasive brain stimulation for motor recovery after stroke. Curr. Opin. Neurol. 30, 388–397. https://doi.org/10.1097/wco.0000000000000462.
Kuceyeski, A.F., Jamison, K.W., Owen, J.P., Raj, A., Mukherjee, P., 2019. Longitudinal increases in structural connectome segregation and functional connectome integration are associated with better recovery after mild TBI. Hum. Brain Mapp. 40, 4441–4456. https://doi.org/10.1002/hbm.24713.
Lin, Q., Liu, J., Zheng, Y., Liang, H., Calhoun, V.D., 2010. Semiblind spatial ICA of fMRI using spatial constraints. Hum. Brain Mapp. 31, 1076–1088. https://doi.org/10.1002/hbm.20919.
Lloyd, S., 1982. Least squares quantization in PCM. Ieee T Inform Theory 28, 129–137. https://doi.org/10.1109/tit.1982.1056489.
Lotze, M., Markert, J., Sauseng, P., Hoppe, J., Plewnia, C., Gerloff, C., 2006. The role of multiple contralesional motor areas for complex hand movements after internal capsular lesion. J. Neurosci. 26, 6096–6102. https://doi.org/10.1523/jneurosci.4564-05.2006.
Madhyastha, T.M., Askren, M.K., Boord, P., Grabowski, T.J., 2015. Dynamic connectivity at rest predicts attention task performance. Brain Connect. 5, 45–59. https://doi.org/10.1089/brain.2014.0248.
Meer, M.P.A. van, Marel, K. van der, Wang, K., Otte, W.M., Bouazati, S. el, Roeling, T.A. P., Viergever, M.A., Sprenkel, J.W.B. van der, Dijkhuizen, R.M., 2010. Recovery of Sensorimotor Function after Experimental Stroke Correlates with Restoration of Resting-State Interhemispheric Functional Connectivity. The Journal of Neuroscience 30, 3964–3972. Doi: 10.1523/jneurosci.5709-09.2010.
Monakow, C. von, 1914. Die Lokalisation im Grosshirn und der Abbau der Funktion durch kortikale Herde. Bergmann JF, Bergmann JF.
Morishita, T., Hummel, F.C., 2017. Non-invasive Brain Stimulation (NIBS) in Motor Recovery After Stroke: Concepts to Increase Efficacy 1–10. Doi: 10.1007/s40473-017-0121-x.
Murase, N., Duque, J., Mazzocchio, R., Cohen, L.G., 2004. Influence of interhemispheric interactions on motor function in chronic stroke. Ann. Neurol. 55, 400–409. https://doi.org/10.1002/ana.10848.
Nowak, D.A., Grefkes, C., Ameli, M., Fink, G.R., 2009. Interhemispheric competition after stroke: brain stimulation to enhance recovery of function of the affected hand. Neurorehabil. Neural Repair 23, 641–656. https://doi.org/10.1177/1545968309336661.
Park, C., Chang, W.H., Ohn, S.H., Kim, S.T., Bang, O.Y., Pascual-Leone, A., Kim, Y.-H., 2011. Longitudinal changes of resting-state functional connectivity during motor recovery after stroke. Stroke 42, 1357–1362. https://doi.org/10.1161/strokeaha.110.596155.
Paul, T., Hensel, L., Rehme, A.K., Tscherpel, C., Eickhoff, S.B., Fink, G.R., Grefkes, C., Volz, L.J., 2021. Early motor network connectivity after stroke: an interplay of general reorganization and state-specific compensation. Hum. Brain Mapp. 42, 5230–5243. https://doi.org/10.1002/hbm.25612.
Perez, M.A., Cohen, L.G., 2008. Mechanisms underlying functional changes in the primary motor cortex ipsilateral to an active hand. J. Neurosci. 28, 5631–5640. https://doi.org/10.1523/jneurosci.0093-08.2008.
Power, J.D., Cohen, A.L., Nelson, S.M., Wig, G.S., Barnes, K.A., Church, J.A., Vogel, A.C., Laumann, T.O., Miezin, F.M., Schlaggar, B.L., Petersen, S.E., 2011. Functional network organization of the human brain. Neuron 72, 665–678. https://doi.org/10.1016/j.neuron.2011.09.006.
Rabany, L., Brocke, S., Calhoun, V.D., Pittman, B., Corbera, S., Wexler, B.E., Bell, M.D., Pelphrey, K., Pearlson, G.D., Assaf, M., 2019. Dynamic functional connectivity in schizophrenia and autism spectrum disorder: Convergence, divergence and classification. Neuroimage Clin 24, 101966. https://doi.org/10.1016/j.nicl.2019.101966.
Rachakonda, S., Egolf, Correa, Calhoun, 2007. Group ICA of fMRI toolbox (GIFT) manual [WWW Document]. URL file:///Users/lukashensel/Downloads/v1.3h_GIFTManual.pdf (accessed 8.2.22).
Rehme, A.K., Eickhoff, S.B., Grefkes, C., 2013. State-dependent differences between functional and effective connectivity of the human cortical motor system. Neuroimage 67, 237–246. https://doi.org/10.1016/j.neuroimage.2012.11.027.
Rice, N.J., Tunik, E., Grafton, S.T., 2006. The anterior intraparietal sulcus mediates grasp execution, independent of requirement to update: new insights from transcranial magnetic stimulation. J. Neurosci. 26, 8176–8182. https://doi.org/10.1523/jneurosci.1641-06.2006.

Rousseeuw, P.J., 1987. Silhouettes: a graphical aid to the interpretation and validation of cluster analysis. J. Comput. Appl. Math. 20, 53–65. https://doi.org/10.1016/0377-0427(87)90125-7.

Rushworth, M.F.S., Walton, M.E., Kennerley, S.W., Bannerman, D.M., 2004. Action sets and decisions in the medial frontal cortex. Trends Cogn. Sci. 8, 410–417. https://doi.org/10.1016/j.tics.2004.07.009.

Sakoğlu, Ü., Pearlson, G.D., Kiehl, K.A., Wang, Y.M., Michael, A.M., Calhoun, V.D., 2010. A method for evaluating dynamic functional network connectivity and task-modulation: application to schizophrenia. Magnet. Reson. Mater. Phys. Biol. Med. 23, 351–366. https://doi.org/10.1007/s10334-010-0197-8.

Salman, M.S., Du, Y., Lin, D., Fu, Z., Fedorov, A., Damaraju, E., Sui, J., Chen, J., Mayer, A.R., Posse, S., Mathalon, D.H., Ford, J.M., Erp, T.V., Calhoun, V.D., 2019. Group ICA for identifying biomarkers in schizophrenia: 'Adaptive' networks via spatially constrained ICA show more sensitivity to group differences than spatio-temporal regression. Neuroimage Clin. 22, 101747. https://doi.org/10.1016/j.nicl.2019.101747.

Schulz, R., Buchholz, A., Frey, B.M., Bönstrup, M., Cheng, B., Thomalla, G., Hummel, F. C., Gerloff, C., 2016. Enhanced effective connectivity between primary motor cortex and intraparietal sulcus in well-recovered stroke patients. Stroke 47, 482–489. https://doi.org/10.1161/strokeaha.115.011641.

Schwanenflug, N. von, Krohn, S., Heine, J., Paul, F., Prüss, H., Finke, C., 2022. State-dependent signatures of anti-N-methyl-d-aspartate receptor encephalitis. Brain Commun. 4. https://doi.org/10.1093/braincomms/fcab298 fcab298.

Seeley, W.W., Menon, V., Schatzberg, A.F., Keller, J., Glover, G.H., Kenna, H., Reiss, A.L., Greicius, M.D., 2007. Dissociable intrinsic connectivity networks for salience processing and executive control. J. Neurosci. 27, 2349–2356. https://doi.org/10.1523/jneurosci.5587-06.2007.

Shine, J.M., Bissett, P.G., Bell, P.T., Koyejo, O., Balsters, J.H., Gorgolewski, K.J., Moodie, C.A., Poldrack, R.A., 2016. The dynamics of functional brain networks: integrated network states during cognitive task performance. Neuron 92, 544–554. https://doi.org/10.1016/j.neuron.2016.09.018.

Steiner, L., Homan, S., Everts, R., Federspiel, A., Kamal, S., Rodriguez, J.A.D., Kornfeld, S., Slavova, N., Wiest, R., Kaelin-Lang, A., Steinlin, M., Grunt, S., 2021. Functional connectivity and upper limb function in patients after pediatric arterial ischemic stroke with contralateral corticospinal tract wiring. Sci. Rep. 11, 5490. https://doi.org/10.1038/s41598-021-84671-2.

Stinear, C.M., Barber, P.A., Smale, P.R., Coxon, J.P., Fleming, M.K., Byblow, W.D., 2007. Functional potential in chronic stroke patients depends on corticospinal tract integrity. Brain 130, 170–180. https://doi.org/10.1093/brain/awl333.

Tibshirani, R., Walther, G., Hastie, T., 2001. Estimating the number of clusters in a data set via the gap statistic. J. R. Stat. Soc. Ser. B (Stat Methodol.) 63, 411–423.

Tscherpel, C., Hensel, L., Lemberg, K., Freytag, J., Michely, J., Volz, L.J., Fink, G.R., Grefkes, C., 2020a. Age affects the contribution of ipsilateral brain regions to movement kinematics. Hum. Brain Mapp. 41, 640–655. https://doi.org/10.1002/hbm.24829.

Tscherpel, C., Hensel, L., Lemberg, K., Vollmer, M., Volz, L.J., Fink, G.R., Grefkes, C., 2020b. The differential roles of contralesional frontoparietal areas in cortical reorganization after stroke. Brain Stimul. 13, 614–624. https://doi.org/10.1016/j.brs.2020.01.016.

Turton, A., Wroe, S., Trepte, N., Fraser, C., Lemon, R.N., 1996. Contralateral and ipsilateral EMG responses to transcranial magnetic stimulation during recovery of arm and hand function after stroke. Electroencephalogr. Clin. Neurophysiol. Electromyogr. Mot. Control 101, 316–328. https://doi.org/10.1016/0924-980x(96)95560-5.

Vergara, V.M., Abrol, A., Calhoun, V.D., 2019. An average sliding window correlation method for dynamic functional connectivity. Hum. Brain Mapp. 40, 2089–2103. https://doi.org/10.1002/hbm.24509.

Vicentini, J.E., Weiler, M., Casseb, R.F., Almeida, S.R., Valler, L., de Campos, B.M., Li, L. M., 2021. Subacute functional connectivity correlates with cognitive recovery six months after stroke. Neuroimage Clin. 29, 102538. https://doi.org/10.1016/j.nicl.2020.102538.

Volz, L.J., Rehme, A.K., Michely, J., Nettekoven, C., Eickhoff, S.B., Fink, G.R., Grefkes, C., 2016. Shaping early reorganization of neural networks promotes motor function after stroke. Cereb. Cortex 26, 2882–2894. https://doi.org/10.1093/cercor/bhw034.

Volz, L.J., Vollmer, M., Michely, J., Fink, G.R., Rothwell, J.C., Grefkes, C., 2017. Time-dependent functional role of the contralesional motor cortex after stroke. NeuroImage. Clinical 16, 165–174. https://doi.org/10.1016/j.nicl.2017.07.024.

Wang, L., Yu, C., Chen, H., Qin, W., He, Y., Fan, F., Zhang, Y., Wang, M., Li, K., Zang, Y., Woodward, T.S., Zhu, C., 2010. Dynamic functional reorganization of the motor execution network after stroke. Brain 133, 1224–1238. https://doi.org/10.1093/brain/awq043.

Ward, N.S., 2017. Restoring brain function after stroke — bridging the gap between animals and humans. Nat. Rev. Neurol. 13, 244–255. https://doi.org/10.1038/nrneurol.2017.34.

Ward, N.S., Brown, M.M., Thompson, A.J., Frackowiak, R.S.J., 2003. Neural correlates of motor recovery after stroke: a longitudinal fMRI study. Brain 126, 2476–2496. https://doi.org/10.1093/brain/awg245.

Werhahn, K.J., Conforto, A.B., Kadom, N., Hallett, M., Cohen, L.G., 2003. Contribution of the ipsilateral motor cortex to recovery after chronic stroke. Ann. Neurol. 54, 464–472. https://doi.org/10.1002/ana.10686.

Wiesendanger, M., 2006. Constantin von Monakow (1853-1930): a pioneer in interdisciplinary brain research and a humanist., Comptes rendus biologies. Doi: 10.1016/j.crvi.2006.03.011.

Wu, K., Jelfs, B., Neville, K., Mahmoud, S.S., He, W., Fang, Q., 2024. Dynamic reconfiguration of brain functional network in stroke. IEEE J. Biomed. Heal. Inform. 28, 3649–3659. https://doi.org/10.1109/jbhi.2024.3371097.